Mon. Not. R. Astron. Soc. **000**, 1–9 (2006) Printed 10 August 2006 (MN LATEX style file v2.2)

Star formation triggered by SN explosions: an application to the stellar association of β Pictoris

C. Melioli[1⋆], E. M. de Gouveia Dal Pino[1]†, R. de la Reza[2]‡, A. Raga[3]§
[1] *Universidade de São Paulo, IAG, Rua do Matão 1226, Cidade Universitária, São Paulo 05508-900, Brazil*
[2] *Observatório Nacional, Rua General José Cristino 77, São Cristovão, 20921-400 Rio de Janeiro, Brazil*
[3] *Instituto de Ciencias Nucleares, Universidad Nacional Autónoma de México, Ap.P. 70543, 04510 DF, Mexico*

Accepted ??? ???. Received ??? ???; in original form ??? ??? ???

ABSTRACT

In the present study, considering the physical conditions that are relevant in interactions between supernova remnants (SNRs) and dense molecular clouds for triggering star formation we have built a diagram of SNR radius versus cloud density in which the constraints above delineate a shaded zone where star formation is allowed. We have also performed fully 3-D radiatively cooling numerical simulations of the impact between SNRs and clouds under different initial conditions in order to follow the initial steps of these interactions. We determine the conditions that may lead either to cloud collapse and star formation or to complete cloud destruction and find that the numerical results are consistent with those of the SNR-cloud density diagram. Finally, we have applied the results above to the $\beta-$Pictoris stellar association which is composed of low mass Post-T Tauri stars with an age of 11 Myr. It has been recently suggested that its formation could have been triggered by the shock wave produced by a SN explosion localized at a distance of about 62 pc that may have occurred either in the Lower Centaurus Crux (LCC) or in the Upper Centaurus Lupus (UCL) which are both nearby older subgroups of that association (Ortega and co-workers). Using the results of the analysis above we have shown that the suggested origin for the young association at the proposed distance is plausible only for a very restricted range of initial conditions for the parent molecular cloud, i.e., a cloud with a radius of the order of 10 pc and density of the order of 20 cm^{-3} and a temperature of the order of 50−100 K.

Key words: stellar clusters: general — stellar cluster: ISM, SNe

1 INTRODUCTION

The young Beta Pictoris Association is a nearby unbound moving group formed by low-mass post-T Tauri stars. Its mean distance to the Sun is ~ 35 pc (Zuckerman et al. 2001; Torres et al. 2006). Due to its age ($\sim$ 12 Myr, Zuckerman et al. 2001; or 11.2 $\pm$ 0.3 Myr, Ortega et al. 2002, 2004), this association has received a lot of attention, since it can be the host of planetary formation among its star members. Also, this group contains the largest number of debris disks and very probably the oldest classical T Tauri type disk (Torres et al. 2006). Distinctly from the mechanism usually proposed for star formation in open clusters, Ortega et al. (2002, 2004) have suggested that a type II supernova could have triggered the formation of this loose group of stars. That could also be the case for the younger association of TW Hya 8 Myr ago (de la Reza et al. 2006).

A star formation process starts when a pressure-bounded, self-gravitating cloud or clump becomes gravitationally unstable. In the classical theory developed by Jeans, an instability occurs when the gravitational attraction overcomes the combined action of all dispersive and resistive forces. The simplest case is a system in virial equilibrium where only the presence of the potential energy is considered. If the potential energy is greater than twice the total kinetic energy, the system collapses, while in the opposite case, it expands. This consideration can be extended by including any relevant additional physical forces acting on the gas.

It has long been known that essentially all present day star formation takes place in giant molecular clouds (GMCs, e.g. Blitz 1993, Williams, Blitz, & McKee 2000), so that it is

⋆ cmelioli@astro.iag.usp.br
† dalpino@astro.iag.usp.br
‡ delareza@on.br
§ raga@nuclecu.unam.mx

vital to understand the properties, dynamical evolution and fragmentation of these clouds in order to understand star formation.

There are several possible ways of driving a cloud or clump to collapse, but at the present time is not well understood how a self-gravitating cloud becomes gravitationally unstable. GMCs are observed to contain a wealth of structures on all length scales with highly supersonic motions (Larson 1981; Blitz & Williams 1999; Elmegreen & Scalo 2004). Based on numerical simulations, a number of authors have argued that it is these supersonic motions, maintained by internal or external driving mechanisms, that induce the observed density inhomogeneities in the gas (Mac Low & Klessen 2004; Elmegreen & Scalo 2004), and that it is therefore the supersonic motions that drive star formation. Suggested candidates for an internal driving mechanism include feedback from low-mass star formation although GMCs with and without star formation have similar kinematic properties (Williams, Blitz & McKee 2000). External candidates include galactic spiral shocks (Roberts 1969, Bonnell et al. 2006) and supernova and superbubble shocks (Wada & Norman 2001; Elemegreen & Scalo 2004). All of these processes seem to have sufficient energy to explain the kinematics of the ISM and can generate the observed velocity dispersion-sizescale relation (Kornreich & Scalo 2000). Other mechanisms, such as protostellar winds and jets, magnetorotational instabilities, expansion of H II regions and fluctuations in the UV field apparently inject energy into the ambient medium at a rate which is about an order of magnitude lower than the energy that is required to explain the random motions of the ISM at several scales.

Here we focus on one of these driving mechanisms and investigate the possibility that a SN that exploded in the recent past produced a shock front that compressed a molecular cloud and induced the formation of the β Pictoris association, as suggested by Ortega et al. (2002, 2004). [1]

In §2, we consider the equations that are relevant for a SNR expansion and the equations that describe the interaction between an expanding SNR and a molecular cloud. In §3, we obtain analytically a set of constraints from these interactions that may lead to star formation and build a diagram where these constraints approximately delineate a zone in the parameter space which is appropriate for star formation. In §4, we apply these analytical results to the physical conditions that could have led to the formation of the β Pictoris association induced by a SNR-cloud interaction and also describe radiatively cooling 3-D hydrodynamical simulations of the interactions between a SNR and a molecular cloud considering initial conditions which are appropriate to the β Pictoris environment and find that the results confirm those obtained from the analytical study. In §5 we draw our conclusions.

[1] We notice that a more general study of the role that SN explosions play on the process of structure and star formation and on the generation of turbulence in the ISM of normal and starburst galaxies will be presented elsewhere (Melioli et al. 2006).

2 SNR EVOLUTION AND SHOCK WAVE-CLOUD INTERACTIONS

2.1 Conditions of the SNR

A type II supernova explosion generates a spherical shock wave that sweeps the interstellar medium (ISM), leading to the formation of a supernova remnant (SNR). The interaction between a SNR and a cloud may compress the gas sufficiently to drive the collapse of the cloud. The kinetic energy associated to a SN event is of the order of 10^{51} erg, the ejected mass into the ISM is $M_{ej} \simeq 10$ M$_\odot$ and its terminal velocity is $\sim 10^4$ km s^{-1}. This ejected mass will expand at nearly constant velocity until it encounters a comparable mass of ambient medium. This occurs at a time t_{sh} which determines the onset of the SNR formation (e.g., McCray 1985):

$$t_{sh} = \frac{200}{n^{1/3}} \left(\frac{M_{ej}}{M_\odot} \right)^{1/3} \quad \text{yr} \tag{1}$$

where n is the ambient number density in cm^{-3}. The SNR evolution is characterized by two phases: an adiabatic (or *Sedov-Taylor*) phase and a radiative phase. In the adiabatic phase the radius, R_{snr}, and the expansion velocity , v_{snr}, of the SNR are, respectively:

$$R_{snr}(t) \sim 13 \left(\frac{E_{51}}{n} \right)^{1/5} t_4^{2/5} \quad \text{pc} \tag{2}$$

$$v_{snr}(t) \sim 508 \left(\frac{E_{51}}{n} \right)^{1/5} t_4^{-3/5} \quad \text{km/s} \tag{3}$$

where E_{51} is the initial SN energy in units of 10^{51} erg and t_4 is the time in units of 10^4 yr. Using Eqs. 1 and 2, we obtain:

$$v_{snr}(R) \sim 68 \left(\frac{E_{51}}{n} \right)^{0.5} \frac{1}{R_{snr,50}^{1.5}} \quad \text{km/s} \tag{4}$$

where $R_{snr,50}$ is the radius of the SNR in units of 50 pc. The effects of the radiative losses become important at a time (McCray 1985):

$$t_{cool} = 3 \times 10^4 \ {E_{51}}^{0.22} \ n^{-0.55} \quad \text{yr} \tag{5}$$

after which the SNR enters the radiative phase and its evolution in the ISM is then described by:

$$R_{snr}(t) \sim 19 \ \frac{E_{51}^{0.23}}{n^{0.26}} \ t_4^{2/7} \quad \text{pc} \tag{6}$$

$$v_{snr}(t) \sim 530 \ \frac{E_{51}^{0.23}}{n^{0.26}} \ t_4^{-5/7} \quad \text{km/s} \tag{7}$$

From Eqs. 6 and 7 we obtain:

$$v_{snr}(R) \sim 47 \ \frac{E_{51}^{0.8}}{n^{0.91} \ R_{snr,50}^{5/2}} \quad \text{km/s} \tag{8}$$

When the internal pressure of the SNR becomes comparable to the ISM pressure, it stalls, fragments and the hot gas that fills the SNR begins to mix with the ISM. Assuming that the radiative losses of the hot gas are negligible, this phase is expected to occur when:

$$R_{snr} \sim 56 \ T_4^{-0.2} \ {E_{51}}^{0.12} \ n^{-0.37} \quad \text{pc} \tag{9}$$

where T_4 is the ISM temperature in units of 10^4 K.

2.2 Conditions for a SNR-cloud interaction

Molecular clouds are dominated by molecular H_2 because they are opaque to the UV radiation that elsewhere dissociates the molecules. The heating and cooling processes in molecular clouds are due mainly to the presence of molecules composed of heavier elements such as carbon, nitrogen, and oxygen. Emission line observations reveal clumps and filaments on all scales. While the GMCs have masses of 10^5 to 10^6 $M_\odot$ and extend over a few $\sim$ 10 pc, the smallest embedded structures are protostellar cores with masses of a few solar masses or less and sizes smaller than 0.1 pc. The cloud temperature typically ranges from 10 K to 100 K and only in the presence of a photo-ionizing source it increases to 10^4 K. If we assume a homogeneous cloud with constant density and temperature, we can describe its evolution after an interaction with a SNR shell moving at a supersonic velocity.

After the impact, an internal forward shock propagates into the cloud with a velocity v_{cs}. The ram pressure of the blast wave, $\sim n_{sh} v_{snr}^2$, must be comparable to the ram pressure behind the shock in the cloud, $\sim n_c v_{cs}^2$ and this results in:

$$v_{cs,A} \sim v_{snr} \left(\frac{n_{sh}}{n_c}\right)^{0.5} = \frac{43\ E_{51}^{0.5}}{R_{snr,50}^{1.5}\ n_{c,10}^{0.5}} \quad \mathrm{km/s} \qquad (10)$$

in the adiabatic case, where $n_{c,10}$ is the cloud density in units of 10 cm^{-3} and where we have assumed $n_{sh} = 4n$ (as appropriate for a strong adiabatic shock), and

$$v_{cs,R} \sim f_{10}^{0.5}\ \frac{46\ E_{51}^{0.8}}{R_{snr,50}^{5/2}\ n_{c,10}^{0.5}\ n^{0.41}} \quad \mathrm{km/s} \qquad (11)$$

in the radiative case, where f_{10} is the density contrast between the shell and the ISM density, in units of 10.

The equations above are valid for a planar shock. For spherical cloud-SNR interactions, the effects of curvature in the shock should be considered. The instantaneous velocity of the shocked gas moving towards the center of the cloud is only a fraction of the SNR velocity and depends on the density contrast χ between the shell and the cloud (as in the planar shock case) and the angle γ between the SNR velocity vector and the line that links the center of the cloud and the instantaneous contact point between the cloud and the SNR (see Figure 1). When the SNR touches the cloud, these two lines are coincident ($\gamma = 0$) and $v_{cs} = \chi^{0.5} V_{snr}$. Later, when the SNR crosses the center of the cloud, $\gamma = \pi/2$, and $v_{cs} = 0$. The average value of the velocity integrated over the SNR crossing time, $t_{c,snr}$ is:

$$\hat{v}_{cs} = v_{snr} \left(\frac{n_{sh}}{n_c}\right)^{0.5} \frac{1}{t_{c,snr}} \int_0^{t_{c,snr}} cos\gamma(t)\ dt \qquad (12)$$

where $t_{c,snr} = 2R_c/v_{snr}$.
From Figure 1 we find that:

$$\gamma(t) = \alpha(t) + \beta(t)$$

where:

$$\alpha(t) = cos^{-1}(1 - \frac{v_{snr} t}{r_c})$$

$$\beta(t) = sen^{-1}[\frac{(2v_{snr} r_c t - v_{snr}^2 t^2)^{0.5}}{R_{snr}}]$$

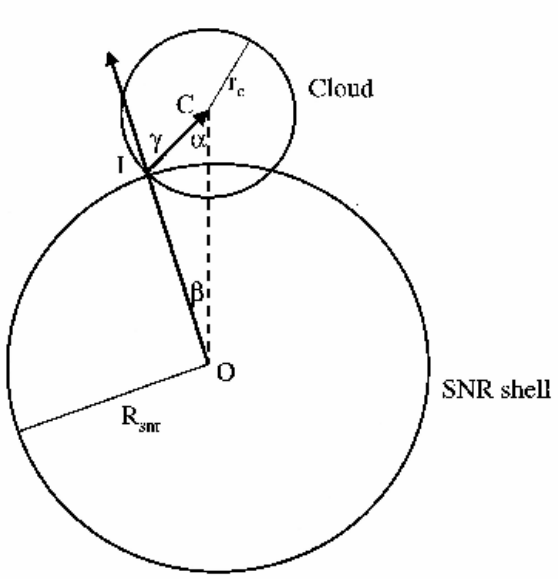

Figure 1. Schematic diagram of the interaction between a SNR and a cloud. The SNR expands and impacts the cloud. The angles α, β and γ are functions of the time, the SNR velocity and the cloud and SNR radii, as indicated by the equations of the text.

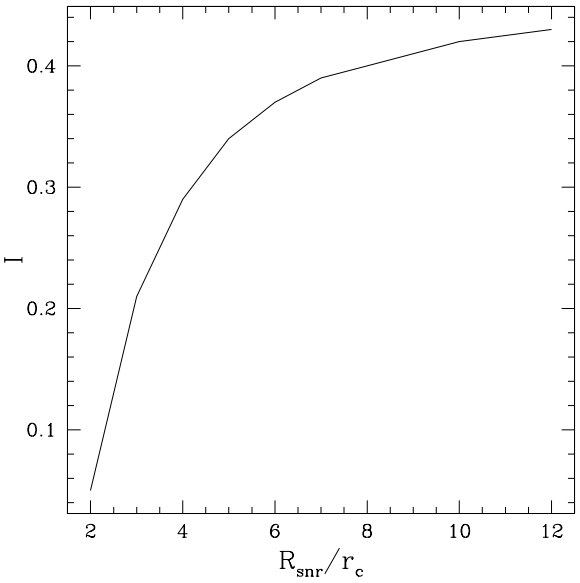

Figure 2. Values of I for different ratios R_{SNR}/r_c

and r_c is the cloud radius expressed in pc.

Figure 2 depicts the plot of the integral term ($I = 1/t_{c,snr} \int_0^{t_{c,snr}} cos\gamma(t)\ dt$) of Eq. (15) as a function of the ratio R_{snr}/r_c.
For example, for a SNR with $R_{snr} = 50$ pc and a cloud with $r_c = 10$ pc, we find:

$$\hat{v}_{cs} = 0.34\ (\frac{n_{bw}}{n_c})^{0.5}\ v_{snr} \qquad (13)$$

and the internal shock wave will cross the cloud in a time t_{cc}:

$$t_{cc,A} \sim 7 \times 10^5 \ \frac{n_{c,10}^{0.5} \ r_{c,10} \ R_{snr,50}^{1.5}}{I_5 \ E_{51}^{0.5}} \quad \text{yr} \tag{14}$$

in the case of a SNR in the adiabatic phase, where $r_{c,10}$ is the cloud radius in units of 10 pc and I_5 is the integral I computed for a ratio $R_{snr}/r_c = 5$. In the case of a SNR in the radiative phase, we obtain:

$$t_{cc,R} \sim 7 \times 10^5 \frac{r_{c,10} \ R_{snr,50}^{2.5} \ n_{c,10}^{0.5} \ n^{0.41}}{f_{10}^{0.5} \ E_{51}^{0.8}} \quad \text{yr.} \tag{15}$$

After this time, the shocked gas reaches the center of the cloud, rebounds and, in the absence of the effects of a gravitational field, the compressed cloud may start a re-expansion phase. The equations above imply that when the SNR interacts with a cloud the Mach number of the forward shock propagating into the cloud, is:

$$M_A = 14 \frac{E_{51}^{0.5}}{T_{c,100}^{0.5} \ R_{snr,50}^{1.5} \ n_{c,10}^{0.5} \ I_5} \tag{16}$$

if the SNR at the epoch of the interaction is yet in the adiabatic phase, and

$$M_R = 44 \ \frac{f_{10} \ E_{51}^{0.8} \ I_5}{n_{c,10}^{0.5} \ T_{c,100}^{0.5} \ R_{snr,50}^{2.5} \ n^{0.41}} \tag{17}$$

for an interacting SNR in the radiative phase, where $T_{c,100}$ is the cloud temperature in units of 100 K. [2]

Depending on the physical conditions of the cloud, the propagation of the shock front into it can be either adiabatic or radiative. For the shocked gas at temperatures T $\leqslant 10^4$ K, we find that the radiative cooling time is shorter than the crushing time (see, e.g., Melioli, de Gouveia Dal Pino & Raga 2005) and therefore, we can assume that the forward shock wave propagating into the cloud is approximately radiative. The Rankine-Hugoniot relations for a radiative strong shock (with M $\geqslant$ 10), are:

$$T_{c,sh} = T_c \tag{18}$$

$$n_{c,sh} = M^2 \ n_c \tag{19}$$

where $n_{c,sh}$ and $T_{c,sh}$ are the density and the temperature of the cloud shocked gas, respectively. Using Eqs. (16) and (17), we can then estimate the value for the cloud gas density after the interaction with a SNR, that is:

$$n_{c,sh,A} \sim \frac{1800}{R_{snr,50}^3} \ \frac{E_{51} \ I_5^2}{T_{c,100}} \quad \text{cm}^{-3} \tag{20}$$

for a cloud shocked by a SNR in the adiabatic phase, and

$$n_{c,sh,R} \sim \frac{2300}{R_{snr,50}^5} \ \frac{E_{51}^{1.6} \ I_5^2 \ f_{10}}{T_{c,100} \ n^{0.82}} \quad \text{cm}^{-3} \tag{21}$$

for a cloud shocked by a SNR in the radiative phase.

[2] We note that the choice of the set of equations above that are appropriate to describe a given cloud-SNR interaction, with the determination of whether the SNR is in the adiabatic or in the radiative phase, will strictly depend upon the initial SN energy and the ambient medium conditions at the time when the interaction initiates, which are established by eqs. (2) to (8).

3 THE CONDITIONS FOR STAR FORMATION

3.1 The Jeans mass constraint

In principle, in order to find out the conditions for star formation, the cloud (or clump) mass should be larger than the Jeans mass (Jeans, 1902) which, in the absence of magnetic fields, may be written as:

$$m_J \simeq 1.4 \times 10^{-10} \ \frac{T^{1.5}}{\rho^{0.5}} \quad \text{M}_\odot \tag{22}$$

where ρ is the cloud density in g cm^{-3} and T is the temperature in K. For a cloud shocked by a SNR, this condition may be approximately expressed as (using Eqs. 18, to 21):

$$m_{J,A} \simeq 2200 \ \frac{T_{c,100}^2 \ R_{snr,50}^{1.5}}{I_5 \ E_{51}^{0.5}} \quad \text{M}_\odot \tag{23}$$

if the interacting SNR is still in the adiabatic phase, or

$$m_{J,R} \simeq 2000 \ \frac{T_{c,100}^2 \ R_{snr,50}^{2.5} \ n^{0.41}}{I_5 \ f_{10}^{0.5} \ E_{51}^{0.8}} \quad \text{M}_\odot \tag{24}$$

if the SNR is already in the radiative phase. These conditions may be also expressed in terms of the cloud radius:

$$r_{c,A} \geqslant 12 \frac{T_{c,100}^{2/3} \ R_{snr,50}^{0.5}}{I_5^{1/3} \ n_{c,10}^{1/3} \ E_{51}^{0.17}} \quad \text{pc} \tag{25}$$

for a cloud interaction with an adiabatic SNR, or

$$r_{c,R} \geqslant 11.4 \frac{T_{c,100}^{2/3} \ R_{snr,50}^{0.83} \ n^{0.14}}{I_5^{1/3} \ f_{10}^{0.17} \ E_{51}^{0.27}} \quad \text{pc} \tag{26}$$

for an interaction with a radiative SNR. Under the conditions above the shocked cloud is gravitationally unstable and may, in principle, start to collapse.

3.2 Cloud destruction constraint due to strong SNR impact

On the other hand, another effect may occur. If the SNR-cloud interaction is too strong the cloud can be completely destroyed. To check the conditions for this situation, we should compare the cloud gravitational free-fall timescale, t_{ff}, with the destruction timescale due to a strong impact, t_d. In order to have collapse, the gravitationally unstable mode (with typical time t_{un}) must grow fast enough to become nonlinear within the time scale of the cloud-SNR shock interaction (Nakamura et al. 2005). Previous numerical hydrodynamical simulations performed by several authors under an adiabatic approximation (see, e.g., Klein, McKee & Colella 1994; Poludnenko, Frank & Blackman 2002) have shown that the density of the cloud may drop by a factor 2 in 1.5-2 t_{cc} after the impact with a strong shock front. In the presence of radiative cooling of the shocked gas, this density drops by the same factor in $\sim$ 4-6 t_{cc} (Melioli, de Gouveia Dal Pino & Raga 2005). Thus, in order to have collapse, we assume that should be $t_{un} \leqslant 3t_{cc}$. This implies a Mach number:

$$M \leqslant 14 \ (\frac{n_{c,10}}{T_{c,100}})^{1.16} \ r_{c,10}^3 \tag{27}$$

or

$$R_{snr,A} \geqslant 34 \ \frac{E_{51}^{0.33} \ T_{c,100}^{0.44} \ I_5}{n_{c,10} \ r_{c,10}^2} \quad \text{pc} \tag{28}$$

for the interaction with a SNR in the adiabatic phase, and

$$R_{snr,R} \geqslant 50 \ \frac{E_{51}^{0.33} \ f_{10}^{0.2} \ T_{c,100}^{0.26} \ I_5^{0.4}}{n_{c,10}^{0.7} \ n^{0.17} \ r_{c,10}^{1.2}} \quad \text{pc} \tag{29}$$

for the interaction with a SNR in the radiative phase.

Eqs. (22) to (26) and Eqs. (28) and (29) indicate that a SNR interacting with a cloud should on one side have sufficient energy to induce cloud collapse and on the other side be evolved enough in order to not destroy it. These conditions depend on the radius, density and less strongly on the temperature of the cloud, and also on the ISM density and the initial SN energy.

3.3 Penetration extent of the SNR shock front into the cloud

Besides the constraints above, another effect upon the shock should be considered. When the shock wave starts propagating into the cloud, it is decelerated not only by the cloud material, but also by the decay of its pressure due to radiative cooling. This is a non linear situation because the radiative losses depend on the shocked gas temperature, that in turn depends on the shock velocity and on the shocked cloud density, that in turn is sensitive to the radiative losses. However, using energy conservation arguments, we can at least estimate the approximate time at which the shock propagation will stop within the cloud. At this time (t_{st}), the velocity of the shocked gas in the cloud goes to zero and its pressure must balance that of the upstream un-shocked cloud material. From energy conservation, we find approximately that:

$$\frac{3}{2} n_{c,sh}(0) k_b T_{c,sh}(0) + \frac{1}{2} \mu m_H n_{c,sh}(0) v_{c,sh}(0)^2 \simeq$$

$$\frac{3}{2} n_{c,sh}(t_{st}) k_b T_{c,sh}(t_{st}) + \Lambda[T_{c,sh}(t_{st})] \ n_{c,sh}(t_{st})^2 \ t_{st} \tag{30}$$

where the LHS is the total energy behind the shock into the cloud, immediately after the impact and the RHS is the total energy behind the shock after a time t_{st} when it stops. $\Lambda(T)$ is the shocked gas radiative cooling function (which can be approximated by that of an optically thin gas; see e.g., Dalgarno & McCray 1972). The initial temperature and density of the shocked cloud material are approximately given by the adiabatic values. At t_{st}, $n_{c,sh}(t_{st})$ and $T_{c,sh}(t_{st})$ are obtained from the pressure balance above between shocked and unshocked material in the cloud (with the final density approximately equal to the cloud density). The substitution of these relations into the equation above results:

$$t_{st} \simeq \frac{9}{16} \frac{\mu m_H}{n_c \Lambda} v_{sh,c}^2 \quad \text{s.} \tag{31}$$

This time is used to compute the maximum distance that the shock front (initiated by a given SNR) can travel into the cloud before being stopped. This distance is then compared with the radius of the cloud in order to establish the maximum size (that is, the minimum energy) that the SNR should have in order to generate a shock wave able to sweep all of the cloud before being stalled:

$$R_{snr} \leqslant 75 \frac{E_{51}^{0.33} I_5^{0.66}}{(r_{c,10} \Lambda_{27})^{2/9} n_{c,10}^{0.5}} \quad \text{pc} \tag{32}$$

where Λ_{27} is the cooling function in units of 10^{-27}.

This constraint together with the other limits inferred from Eqs. (9), (25), and (28) have been plotted together in Figure 3 that shows the supernova radius as a function of the initial (unshocked) cloud density for different values of the cloud radius. We note that these different constraints provide a restricted shaded zone where the combination of these parameters creates appropriate conditions for star formation. The Jeans mass constraint derived from Eq. (25) for an interaction with an adiabatic SNR (dashed line) and the cloud shock deceleration constraint derived from Eqs. (30) to (32) (dotted line) determine upper limits for the SNR radius, while the condition for complete cloud destruction after an encounter with an adiabatic SNR derived from Eq. (28) (solid line) determines a lower limit for the SNR radius. We have taken a SNR in the adiabatic phase because it has more stored energy than one with the same characteristics in the radiative phase. Only cloud-SNR interactions with initial physical conditions (r_c, n_c and R_{snr}) lying within the shaded region of the figure (between the solid, dotted and dashed lines) may lead to a process of star formation. [3]

4 AN APPLICATION TO β PICTORIS ASSOCIATION

4.1 SNR-cloud interaction: analytical approach

In order to apply the simple analytical study described above to the young moving group of low-mass Post-T Tauri stars of β Pictoris (or BPMG) we assume, as in Ortega et al. (2004), that a type II SN exploded in the past either in the Lower Centaurus Crux (LCC) or in the Upper Centaurus Lupus (UCL), both subgroups of the OB Sco-Cen association, and triggered the formation of BPMG. The potential position of the SN was obtained by tracing back the past position of the runaway star HIP 46950. Those authors estimated that the nearest possible past position of the SN with respect to the calculated stellar dynamical birthplace of BPMG was of 87 pc. Nevertheless, this distance is somewhat affected by the uncertainty of the radial velocity of the runaway star used (35.0 to 10 km/s; Hoogerwerf et al. 2001) and here we will adopt a more conservative value of ~ 60 pc for the SN-cloud distance. Also, taking an ISM number density of 0.05 cm^{-3} and initial cloud parameters $r_c \simeq 10$ pc, $n_c \simeq 10$ cm^{-3}, and $T_c \simeq 100$ K, which are typical for GMCs (e.g., Cernicharo 1991; Mac Low & Klessen 2004), we find that, for a SN energy of 10^{51} erg, the SNR-cloud interaction would have occurred after $\sim 7 \times 10^4$ yr of the SN explosion (Eq. 2). With a SNR velocity $v_{snr} \simeq 280$ km/s (Eq. (3)), the shock velocity into the cloud would be $\hat{v}_{cs}$, ~ 13 km/s (Eq. 12) and after a time $t_{cc} \sim 7 \times 10^5$ yr (Eq.

[3] We notice that the diagrams of Figure 3 have been built for a fixed temperature $T_c = 100$ K. According to Eqs. (25), (28), and (30-32), they are not very sensitive to this parameter, except for the Jeans mass constraint given by Eq. (25), which implies that the upper limit for $R_{snr} \propto T^{-1.3}$. We further notice that a cloud with a temperature in the range of 10 to 50 K and a radius larger than 10 pc is already Jeans unstable over a large range of densities (5 cm^{-}3) and does not require (according to the equations above) an interaction with a shock wave to trigger star formation.

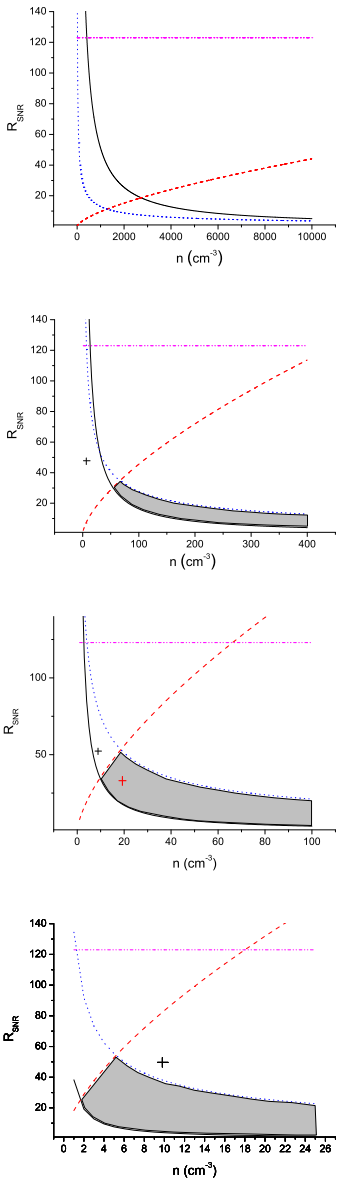

Figure 3. Constraints on the SNR radius versus cloud density for 4 different cloud radius. Top-left panel: $r_c = 1$ pc; top-right panel: $r_c = 5$ pc; bottom-left panel: $r_c = 10$ pc; and bottom-right panel: $r_c = 20$ pc. Solid (black) line: upper limit for complete cloud destruction after an encounter with an adiabatic SNR derived from Eq. 28; dashed (red) line: upper limit for the cloud to reach the Jeans mass derived from Eq. 25 for an interaction with an adiabatic SNR; dotted (blue) line: upper limit for the shock front to travel into the entire cloud before being decelerated to subsonic velocities derived from Eqs. 30 to 34; dotted-dashed (pink) line: maximum radius reached by a SNR in an ISM with density n=0.05 cm^{-3} and temperature T=10^4 K derived from Eq. 9. The shaded area defines the region where star formation can be induced by a SNR-cloud interaction (between the solid, dashed and dotted lines). The crosses in the panels indicate the initial conditions assumed for the clouds in the numerical simulations described in Section 4.2

14), the cloud would be compressed developing a core with shocked material with a density of $n_{c,sh,A} \simeq 1600$ cm^{-3} (Eq. (20)) and temperature $T_{c,sh} \simeq 100$ K (Eq. (18)). However, in order to reach the Jeans mass, the initial radius of the cloud should be (according to Eq. 25), $r_c \geqslant 12.5$ pc, which is larger than the initial radius above and therefore, it indicates that the proposed SNR-cloud interaction is unable to develop a gravitationally unstable system, at least under the initial conditions above. Moreover, we notice that the shock front into the cloud should be highly decelerated under such conditions, and that its average velocity would be $\sim v_{c,sh}/3 \sim 4$ km s^{-1}. Also, we estimate that after the interaction with the SNR, the final density of the shocked cloud material will drop to $\sim n_{c,sh}/9 \sim 170$ cm^{-3}, and in order to reach the Jeans mass condition the initial radius of the cloud should be $r_c \sim 18$ pc. On the other hand, back-tracing of the motion of the Beta-Pictoris members indicate that they may have dispersed from a region of radius $\sim 15 - 24$ pc (Song et al. 2003, Ortega et al. 2002, 2004). If we then take for the progenitor cloud an initial radius of ∼18 pc or larger as indicated above, we find that the forward shock wave is unable to sweep the entire cloud before stalling (Eq. 32), and therefore, also in these cases, the SNR-cloud interaction would be not efficient enough to develop a process of star formation.

4.2 SNR-cloud interaction: numerical simulations

In order to check the semi-analytical estimates above, we have also performed fully 3-D hydrodynamical radiatively cooling simulations employing an unmagnetized modified version of the adaptative grid code YGUAZU (Raga, Navarro-González & Villagrán-Muniz 2000; Raga et al. 2002; Masciadri et al. 2002, Melioli, de Gouveia Dal Pino & Raga 2005) which solve the gas dynamical equations together with a set of continuity equations for several atomic/ionic species (see details in Raga et al. 2002). The computational box has dimensions 102 pc × 56 pc × 56 pc, corresponding to 256 × 128 × 128 grid points at the highest grid level for the first three cases, and to 512 × 256 × 256 grid points for the last case. A SN explosion with energy $E_O = 10^{51}$ is initially injected from the left-bottom corner of the box.

The numerical results are consistent with the previous analytical results. Figure 4a depicts the initial interaction between a SNR and a cloud with radius $r_c = 10$ pc, at a time t= 8×10^4 yr (which is comparable with the one estimated in the analytical study). The initial conditions for this case represent the cross in Figure 3 (bottom-left) which is outside of the shaded area. The SNR shell in Figure 4a has a density ~ 3.5 times the ambient density and its velocity at the moment of the interaction is of 240 km/s. The forward shock wave produced into the cloud (Figure 4b) has a density $n_{c,sh} \sim 100$ cm^{-3}, a temperature $T_{c,sh} \sim 60$ K and a velocity $\hat{v}_{cs} \sim 5$ km s^{-1}. After a time of 3.7 $\times 10^6$ yr from the start of the SNR-cloud interaction, the cloud is compressed in a cylindrical core with a radius of ~ 4 pc, an height of ~ 3 pc, a density of ~ 220 cm^{-3} and temperature of ~ 48 K (Figure 4c). At this point, the cloud core may collapse by its self-gravity or rebound and start a re-expansion of the cloud material. In order to collapse its mass should be larger than the Jeans mass. From Eq. (22), this mass should be $M_j \simeq 2140$ M$_\odot$, while the core mass

inferred from the simulation is $M_c \sim 950$ M$_\odot$. The cloud mass at the beginning of the simulation was $M_c = 1315$ M$_\odot$, and this means that a mass ~ 400 M$_\odot$ has been dragged by the SNR shell (see, e.g., the mass loss rate predicted by Klein, McKee & Colella 1994), and that the shocked cloud is not gravitationally unstable. After reaching a maximum density and occupying a minimum volume, the gas begins to re-expand into the ambient medium, and no dense structure develops (see Figure 4d).

We have also examined the cases of interactions between a SNR and a cloud with a radius of 5 pc and 20 pc. In both cases, as indicated by the crosses marked in Figure 3 (second and third panels, respectively), the interactions are also unable to create the conditions to produce a Jeans unstable cloud core. In the first case (r_c=5 pc, Figure 5) the cloud is swept by the shock front and no core survives after the interaction. In the second case ($r_c = 20$ pc, Figure 6), the shock wave has insufficient energy to sweep all of the gas, and after a few Myrs it stalls within the cloud with a velocity ~ 0 (Figure 6, bottom-right panel). We note that in this case the shocked cloud material does not reach the conditions to become Jeans unstable, but the dense cold shell that develops in the cloud may fragment and eventually generate dense cores, as observed in most GMC.

Finally, we have also examined the interaction between a SNR and a GMC having physical conditions which according to Figure 3 would be able to generate a Jeans unstable core ($r_c = 10$ pc, $n_c = 20$ cm^{-3}, $R_{SNR} = 30$ pc) (see the cross within the shaded area in Figure 3, bottom-left). This simulation was run with a maximum resolution of 0.2 pc, that is twice of that adopted in the other simulations. The evolution of the interacting system (Figure 7) indicates that after ~ 4 Myr a cold and dense cylindrical core develops with radius of ~ 3 pc, height of ~ 3 pc, density $n_{c,sh} \simeq 440$ cm^{-3}, temperature $T_{c,sh} \simeq 40$ K and a total mass of ~ 1200 M$_\odot$. In this case the Jeans mass (Eq. (22)) is ~ 1000 M$_\odot$ and therefore the conditions of the shocked gas are sufficient to form a gravitationally unstable core. This is in agreement with the analytical results of Figure 3, but we note that in this case, the distance between the SNR and the cloud is only 30 pc, that is, much shorter than the proposed distance for the SN-β Pictoris system by Ortega et al. (2002, 2004).

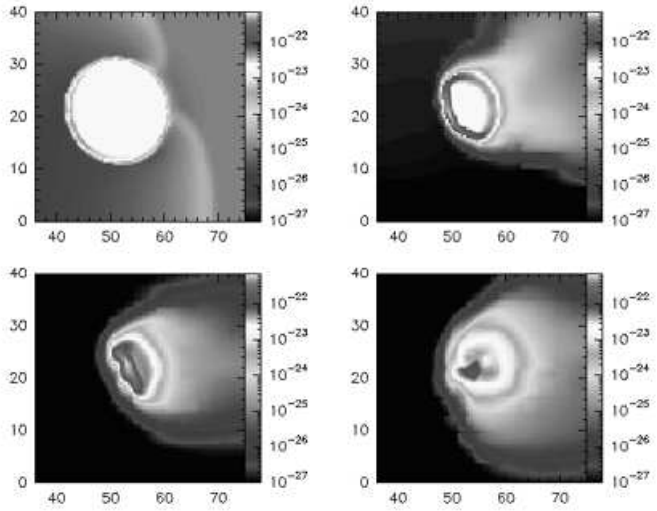

Figure 4. Color-scale maps of the midplane density distribution (in log scale) evolution of the interaction between an expanding SNR and a cloud at a time a) $t = 2.2 \times 10^5$ yr (top-left); b) $t = 2. \times 10^6$ yr (top-right); c) $t = 3.7 \times 10^6$ yr (bottom-left); and d) $t = 8.5 \times 10^6$ yr (bottom-right). The SNR is generated by a SN explosion with an energy of 10^{51} erg. The ISM where the SNR expands has a number density $n = 0.05$ cm^{-3}, and a temperature 10^4 K. The cloud has an initial number density $n_c = 10$ cm^{-3}, temperature $T_c = 100$ K, and radius $r_c = 10$ pc. The initial distance between the external surface of the cloud and the center of the SNR is 62 pc, as assumed by Ortega et al. (2005).

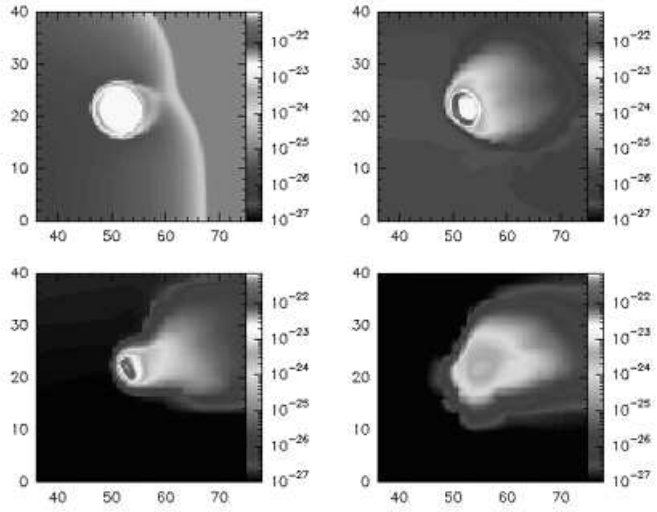

Figure 5. The same as in Figure 4, except that here the cloud has an initial radius $r_c = 5$ pc. The times are: $t = 2.5 \times 10^5$ yr (top-left); $t = 8.9 \times 10^5$ yr (top-right); $t = 1.8 \times 10^6$ yr (bottom-left); $t = 8.5 \times 10^6$ yr (bottom-right).

5 CONCLUSIONS

We have here presented a preliminary study of the role that interactions between SNRs and dense molecular clouds play in the process of star formation.

Considering the physical conditions that are relevant in these interactions for triggering star formation (like the choice of the cloud and SNR initial conditions, the derivation of an appropriate Jeans mass, the determination of the conditions for complete destruction of the cloud after the impact, and the determination of the extent of penetration of the shock front into the cloud) we have built in Section 3, a diagram of the SNR radius versus the cloud density for a fixed cloud radius in which the constraints above delineate a shaded zone where star formation induced by SN shock front-cloud interactions is possible.

We have also performed fully 3-D radiatively cooling numerical simulations of the impact between a SNR and a cloud for different initial conditions (in Section 4) and, although self-gravity has not been included in the present study, we have been able to track the first steps of these interactions and detect the conditions that lead either to cloud collapse and star formation or to complete cloud destruction. We have found that the numerical results are consistent with

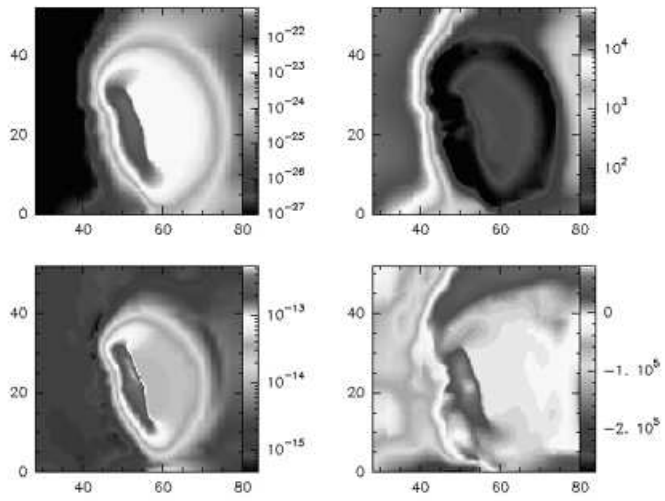

Figure 6. Color log scale maps of the midplane: a) density in cm s^{-3}(top-left); b) temperature in K (top-right); c) pressure in dyne (bottom-left); and velocity distribution in cm s^{-1} (bottom-right) for a cloud with an initial radius $r_c = 20$ pc at a time $t = 8 \times 10^6$ yr. The other initial conditions are the same as in Figure 5.

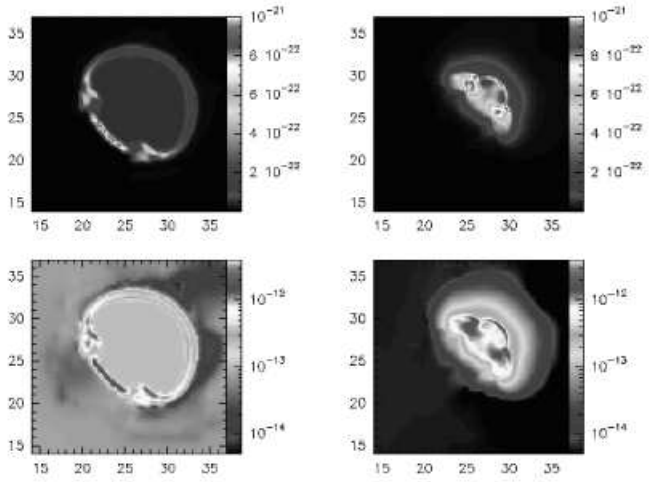

Figure 7. Color log scale maps of the midplane density (upper panels) and pressure distributions (bottom panels) for a cloud with initial density $n_c = 20$ cm^{-3} shocked by a SNR with $R_{SNR} = 30$ pc. The left panels are at a time $t = 1.6 \times 10^6$ yr and the right panels are at $t = 4.1 \times 10^6$ yr.

those established by the SNR-cloud density diagram in spite of the fact that the later have been built from approximate conditions derived from a simplified analytic theory.

Finally, we have applied the results above to the nearby young stellar association $\beta-$ Pictoris which is composed of low mass Post-T Tauri stars with an age of 11 Myr. Ortega et al. (2004) have recently suggested that its formation could have been triggered by the shock wave produced by a SN explosion that may have occurred either in the Lower Centaurus Crux (LCC) or in Upper Centaurus Lupus (UCL) older subgroups of the OB Cen-Sco association. Taking from their study the initial conditions that would be appropriate for both the ISM and the cloud and assuming an interacting SN shock front still in the adiabatic phase, we have found that the suggested origin for the young association by Ortega et al. is implausible, for the proposed distance of the SNR, of ~ 60 pc, unless the parent molecular cloud had a radius of the order of 10 pc and a density of the order of 20 cm^{-3}, as indicated by the shaded zone of the third panel of Figure 3. A larger cloud radius (~ 20 pc) would require a much smaller cloud density (see bottom panel of Figure 3) which would not be much frequent in GMCs with a temperature greater than 50 K. These analytical results have also been confirmed by the numerical simulations (see Figures 5 to 7). The results indicate that, unless the SN had an extremely (unusual) high energy, or had exploded at a much smaller distance than the proposed one (of ~ 60 pc), then the suggested scenario for triggering the formation of the $\beta-$ Pictoris association would be possible only under the restrict conditions above. In fact, our numerical results also revealed that using a similar parent cloud density to that proposed above, but assuming an interaction with a SNR at half the distance (30 pc) and a cloud with larger radius (20 pc) the interaction may lead to the development of structuring and formation of dense cold clumps behind the shock in the cloud, which may eventually aggregate and generate dense Jeans unstable cores, as observed in most GMCs.

We should emphasize that the present study is still preliminary and the results have been mainly focused on the particular conditions of the β Pictoris association and its neighbourhood. Besides, it has been performed without taking into account the presence of magnetic fields. These may also play an important role on star formation as they tend to attain values as large as $\sim 100\mu$G to few mG within the densest cores of the molecular clouds and can dominate over the thermal and turbulent pressures, so that at least the densest clouds may be magnetically supported. A more general investigation of star formation processes induced by SNR shock fronts including not only radiative cooling but also magnetic fields and self-gravity is in preparation and will be presented elsewhere (Melioli et al. 2006)

ACKNOWLEDGMENTS

C.M. and E.M.G.D.P acknowledge financial support from the Brazilian Agencies FAPESP and CNPq. The authors are also indebted to an anonymous referee for his/her careful revision and comments on this work

REFERENCES

Blitz, L., 1993, Protostars and planets III, p. 125
Blitz, L., Williams, J.P., 1999, The Origin of Stars and Planetary Systems. Edited by C.J. Lada & N.D. Kylafis. Kluwer Acad. Publ., p.3
Bonnell, I.A., Dobbs, C.L., Robitaille, T.P. & Pringle, J.E., 2006, MNRAS, 365, 37
Dalgarno, A.& McCray, R.A., 1972, ARA&A, 10, 375
de la Reza, R., Jilinski, G. & Ortega, V.G. 2006 to appear in the AJ (May)
Elmegreen, B.G., & Scalo, J., 2004, ARA&A, 42, 21

Hoogerwerf, R., de Bruijne, J.H.J. & de Zeeuw, P.T. 2001 A&A 365, 49
Jeans, J.H., 1902, Phil. Trans. A., 199, 1
Klein R., McKee C.F. & Colella P., 1994, ApJ, 420, 213
Kornreich, P. & Scalo, J., 2000, ApJ, 531, 366
Larson, R.B., 1981, MNRAS, 194, 809
Mac Low, M-M., & Klessen, R.S., 2004, RvMP, 76, 125
Masciadri E., de Gouveia Dal Pino E.M., Raga A.C. & Noriega-Crespo A., 2002, ApJ, 580, 950
McCray R., 1985, in Spectroscopy of Astrophysical Plasmas, edited by A. Delgarno & D. Layzer, p270
Melioli, C., de Gouveia Dal Pino, E.M., & Raga, A., 2005, A&A, 443, 495
Melioli, C., de Gouveia Dal Pino, E.M., Leão M. R. M., & Raga, A., 2006, in prep.
Nakamura, F., McKee, C.F., Klein, R.I., Fisher, R.T., 2005, astro-ph/0511016
Ortega, V.G., de la Reza, R., Jilinski, E. & Bazzanella, B., 2004, ApJ, 609, 243
Ortega, V.G., de la Reza, R., Jilinski, E. & Bazzanella, B., 2002, ApJ, 575, 75
Poludnenko A.Y., Frank A. & Blackman E.G., 2002, ApJ, 576, 832
Raga A.C., de Gouveia Dal Pino E.M., Noriega-Crespo A., Minnini P.D. & Velázquez P.F., 2002, A&A, 392, 267
Raga A.C., Navarro-González, R., & Villagrán-Muniz, M. 2000, Rev. Mexicana Astron. Astrofis., 36, 67
Roberts, W.W., 1969, ApJ, 158, 123
Torres, C.A.O., Quast, G. R., da Silva, L., de la Reza, R., Melo, C.H.F. & Sterzik, M. 2006 to be submitted to the A&A
Wada, K. & Norman, C.A., 2001, ApJ, 547, 172
Williams, J.P., Blitz, L., McKee, C.F., 2000, Protostars and Planets IV, eds Mannings, V., Boss, A.P., Russell, S.S., p. 97
Zuckerman, B., Song, I., Bessell, M.S. & Webb, R.A., 2001, ApJ, 562, 87

This paper has been typeset from a TEX/ LATEX file prepared by the author.